ACS APPLIED MATERIALS & INTERFACES

Research Article

www.acsami.org

Anion Conductive Aromatic Block Copolymers Containing Diphenyl Ether or Sulfide Groups for Application to Alkaline Fuel Cells

Naoki Yokota,[†,∥,⊥] Hideaki Ono,[†,⊥] Junpei Miyake,[‡,⊥] Eriko Nishino,[⊥,#] Koichiro Asazawa,[⊥,#] Masahiro Watanabe,[‡] and Kenji Miyatake*[,‡,§,⊥]

[†]Interdisciplinary Graduate School of Medicine and Engineering, [‡]Fuel Cell Nanomaterials Center, and [§]Clean Energy Research Center, University of Yamanashi, 4 Takeda, Kofu 400-8510, Japan

[∥]Takahata Precision Japan Co. Ltd., 390 Maemada, Sakaigawa, Fuefuki, Yamanashi 406-0843, Japan

[⊥]Japan Science and Technology Agency, CREST, 4-1-8 Honcho, Kawaguchi, Saitama 332-0012, Japan

[#]Daihatsu Motor Co. Ltd., Frontier Technology R&D Division, 3000 Ryuo, Gamo, Shiga 520-2593, Japan

Supporting Information

ABSTRACT: A novel series of aromatic block copolymers composed of fluorinated phenylene and biphenylene groups and diphenyl ether (QPE-*bl*-5) or diphenyl sulfide (QPE-*bl*-6) groups as a scaffold for quaternized ammonium groups is reported. The block copolymers were synthesized via aromatic nucleophilic substitution polycondensation, chloromethylation, quaternization, and ion exchange reactions. The block copolymers were soluble in organic solvents and provided thin and bendable membranes by solution casting. The membranes exhibited well-developed phase-separated morphology based on the hydrophilic/hydrophobic block copolymer structure. The membranes exhibited mechanical stability as confirmed by DMA (dynamic mechanical analyses) and low gas and hydrazine permeability. The QPE-*bl*-5 membrane with the highest ion exchange capacity (IEC = 2.1 mequiv g^{-1}) exhibited high hydroxide ion conductivity (62 mS cm^{-1}) in water at 80 °C. A noble metal-free fuel cell was fabricated with the QPE-*bl*-5 as the membrane and electrode binder. The fuel cell operated with hydrazine as a fuel exhibited a maximum power density of 176 mW cm^{-2} at a current density of 451 mA cm^{-2}.

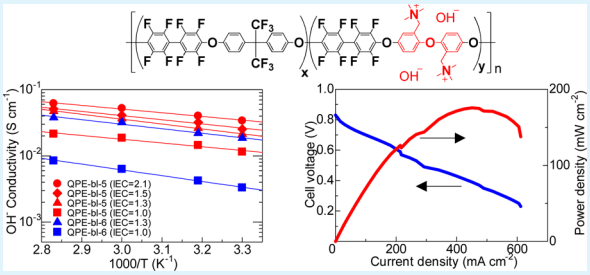

KEYWORDS: *block copolymers, poly(arylene ether), anion conductive membranes, alkaline fuel cells, hydrazine*

INTRODUCTION

Fuel cells are promising energy devices alternative to internal combustion engines due to their high energy conversion efficiency and low environmental burden. Polymer electrolyte fuel cells (PEFCs) using proton exchange membranes (PEMs) have been most extensively developed for the applications in electric vehicles, residential power supplies, and portable devices. Under acidic conditions with PEMs, precious metals such as platinum are required as electrocatalysts, causing a high cost for PEFCs. A potential breakthrough is the use of anion exchange membranes (AEMs).[1−3] Fuel cells with AEMs function under basic conditions and thus possess several advantages over PEFCs, such as a possible use of abundant metal electrocatalysts (Ni, Ag, etc.) and better kinetics of the oxygen reduction reaction. However, the existing AEMs are not as conductive and stable as PEMs, which are major concerns in the development of high performance and durable AEMFCs.

In order to address the issues, a number of AEMs have been developed in recent years.[4−6] We proposed that the multiblock copolymers containing dense ammonium groups in the hydrophilic blocks are highly anion conductive because of distinct hydrophilic/hydrophobic phase separated morphology.[7] Multiblock poly(arylene ether)s containing ammonium-functionalized fluorene groups achieved high hydroxide ion conductivity up to 144 mS cm^{-1} at 80 °C in water. It has been reported that other bulky aromatic groups such as isopropylidene diphenyl[8,9] and tetraphenylmethane[10,11] also served well as a scaffold for ammonium groups. There have been attempts to improve the chemical stability of AEMs. Holdcroft et al. reported that the polymer main chain containing benzimidazolium hydroxide was stable in strong alkaline solution (2 M KOH aq) at 60 °C.[12,13] Hickner et al. reported excellent alkaline stability of a polymer membrane with pendant ammonium groups tethered with long alkyl chains.[14]

In this paper, we report a novel series of AEMs composed of aromatic block copolymers. The objective is to evaluate the effect of diphenyl ether and diphenyl sulfide groups as a scaffold for ammonium groups. Because of the strong electron-donating properties of chalcogen bonds, each phenylene ring could be substituted quantitatively with an ammonium group by the Friedel−Crafts chloromethylation reaction followed by the Menshutkin reaction with trimethylamine, providing high

Received: July 16, 2014
Accepted: September 12, 2014
Published: September 12, 2014

   dx.doi.org/10.1021/am5046586 | ACS Appl. Mater. Interfaces 2014, 6, 17044−17052

ammonium density in the hydrophilic blocks. Furthermore, rather flexible chalcogen bonds could provide AEMs with good solubility in organic solvents. Syntheses, characterization, properties, and fuel cell performance of diphenyl ether (QPE-*bl*-5) and diphenyl sulfide (QPE-*bl*-6) containing AEMs are reported.

EXPERIMENTAL SECTION

Materials. Decafluorobiphenyl (DFBP, > 98.0%, TCI Inc.), hexafluorobisphenol A (HFBPA, > 98.0%, TCI Inc.), bis(4-hydroxyphenyl)sulfide (BHPS, > 98.0%, TCI Inc.), bis(4-hydroxyphenyl)ether (BHPE, > 98.0%, TCI Inc.), potassium carbonate (>99.5%, Kanto Chemical), chloromethyl methyl ether (CMME, > 94.0%, Kanto Chemical), 0.5 M zinc chloride tetrahydrofuran solution (Sigma-Aldrich), 45 wt % trimethylamine aqueous solution (Sigma-Aldrich), methanol (>99.8%, Kanto Chemical), dimethyl sulfoxide (DMSO, > 99.0%, Kanto Chemical), and potassium hydroxide (>86.0%, Kanto Chemical) were commercial products and used as received. *N*,*N*-Dimethylacetamide (DMAc, >99.0%, Kanto Chemical), toluene (>99.5%, Kanto Chemical), and 1,1,2,2-tetrachloroethane (TCE, >97.0%, Kanto Chemical) were dried over 4 Å molecular sieves (Kanto Chemical) prior to use. Chloroform-d_1 with 0.03% TMS (99.8 atom % D, Acros Organics), dimethyl sulfoxide-d_6 with 0.03% TMS (99.9 atom % D, Acros Organics), *N*,*N*-dimethylformamide (DMF, > 99.7%, Kanto Chemical), anhydrous lithium bromide (>95.0%, Kanto Chemical), potassium tetrachloroplatinate (II) (>95.0%, Kanto Chemical), and 60 wt % hydrazine hydrate aqueous solution (Otsuka Chemical) were commercial products and used as received.

Synthesis of DFBP-terminated Telechelic Oligomers 1. A typical procedure is as follows (X = 4). A 100 mL round-bottomed flask equipped with a mechanical stirrer, a reflux condenser, a Dean–Stark trap, and a nitrogen inlet/outlet was charged with HFBPA (2.50 g, 7.44 mmol), potassium carbonate (1.50 g, 11.0 mmol), DMAc (16 mL), and toluene (8 mL). The mixture was stirred at 150 °C for 3 h for azeotropic removal of water with toluene. After the mixture was cooled to room temperature, DFBP (2.98 g, 8.92 mmol) was added to the mixture. The reaction was carried out at 60 °C for 2 h. Then, additional DFBP (0.300 g, 0.892 mmol) as an end-capping reagent was added to the mixture. After the reaction at 60 °C for 1 h, the mixture was cooled to room temperature and diluted with additional DMAc (20 mL). The mixture was poured dropwise into a large excess of deionized water to precipitate a white powder. The crude product was washed with hot deionized water and hot methanol several times. Drying in a vacuum oven at 60 °C gave oligomer **1** (X = 4) in 84% yield.

Synthesis of BHPE-terminated Telechelic Oligomers 2. A typical procedure is as follows (Y = 7). A 100 mL round-bottomed flask equipped with a mechanical stirrer, a reflux condenser, a Dean–Stark trap, and a nitrogen inlet/outlet was charged with BHPE (3.40 g, 16.8 mmol), potassium carbonate (3.50 g, 25.0 mmol), DMAc (30 mL), and toluene (15 mL). The mixture was stirred at 150 °C for 3 h for azeotropic removal of water with toluene. After the mixture was cooled to room temperature, DFBP (4.50 g, 13.5 mmol) was added to the mixture. The reaction was carried out at 60 °C for 2 h. Then, additional BHPE (0.340 g, 1.70 mmol) as an end-capping reagent was added to the mixture. After the reaction at 60 °C for 1 h, the mixture was cooled to room temperature and diluted with additional DMAc (30 mL). The mixture was poured dropwise into a large excess of deionized water to precipitate a white powder. The crude product was washed with hot deionized water and hot methanol several times. Drying in a vacuum oven at 60 °C gave oligomer **2** (Y = 7) in 71% yield.

Synthesis of BHPS-terminated Telechelic Oligomers 3. A typical procedure is as follows (Y = 8). A 100 mL round-bottomed flask equipped with a mechanical stirrer, a reflux condenser, a Dean–Stark trap, and a nitrogen inlet/outlet was charged with BHPS (3.68 g, 16.8 mmol), potassium carbonate (3.50 g, 25.0 mmol), DMAc (30 mL), and toluene (15 mL). The mixture was stirred at 150 °C for 3 h for azeotropic removal of water with toluene. After the mixture was cooled to room temperature, DFBP (4.50 g, 13.5 mmol) was added to the mixture. The reaction was carried out at 60 °C for 2 h. Then, additional BHPS (0.370 g, 1.70 mmol) as an end-capping reagent was added to the mixture. After the reaction at 60 °C for 1 h, the mixture was cooled to room temperature and diluted with additional DMAc (30 mL). The mixture was poured dropwise into a large excess of deionized water to precipitate a white powder. The crude product was washed with hot deionized water and hot methanol several times. Drying in a vacuum oven at 60 °C gave oligomer **3** (Y = 8) in 81% yield.

Synthesis of PE-*bl*-5. A typical procedure is as follows (X = 4, Y = 7). A 100 mL round-bottomed flask equipped with a mechanical stirrer, a reflux condenser, and a nitrogen inlet/outlet was charged with oligomer **1** (2.22 g, 0.480 mmol), oligomer **2** (1.80 g, 0.480 mmol), potassium carbonate (0.100 g, 0.700 mmol), and DMAc (14 mL). After the reaction at 60 °C for 6 h, the mixture was cooled to room temperature and diluted with additional DMAc (20 mL). The mixture was poured dropwise into a large excess of deionized water to precipitate a white powder. The crude product was washed with hot deionized water and hot methanol several times. Drying in a vacuum oven at 60 °C gave PE-*bl*-5 (X = 4, Y = 7) in 90% yield.

Synthesis of PE-*bl*-6. A typical procedure is as follows (X = 4, Y = 8). A 100 mL round-bottomed flask equipped with a mechanical stirrer, a reflux condenser, and a nitrogen inlet/outlet was charged with oligomer **1** (2.08 g, 0.450 mmol), oligomer **3** (2.00 g, 0.450 mmol), potassium carbonate (0.100 g, 0.700 mmol), and DMAc (14 mL). After the reaction at 60 °C for 8 h, the mixture was cooled to room temperature and diluted with additional DMAc (20 mL). The mixture was poured dropwise into a large excess of deionized water to precipitate a white powder. The crude product was washed with hot deionized water and hot methanol several times. Drying in a vacuum oven at 60 °C gave PE-*bl*-6 (X = 4, Y = 8) in 91% yield.

Chloromethylation of the Block Copolymers. A typical procedure is as follows (CMPE-*bl*-5 (X = 4, Y = 7)). A 100 mL pressure bottle equipped with a magnetic stirring bar was charged with PE-*bl*-5 (1.00 g, 0.0556 mmol), 0.5 M zinc chloride tetrahydrofuran solution (2.0 mL, 1.0 mmol), CMME (12.3 mL, 160 mmol), and TCE (21.7 mL) in a glovebox under argon. After the reaction at 80 °C for 120 h, the mixture was cooled to room temperature and diluted with additional TCE. The mixture was poured dropwise into a large excess of methanol to precipitate a white powder. The crude product was washed with methanol several times. Drying in a vacuum oven at 60 °C gave CMPE-*bl*-5 in 84% yield.

Preparation of Quaternized Membranes. CMPE-*bl*-5 (or 6) (0.20 g) was dissolved in TCE (2 mL) and cast onto a flat glass plate. Drying the solution at 50 °C gave a membrane (ca. 50 μm thick). The membrane was immersed in 45 wt % trimethylamine aqueous solution at room temperature for 48 h. The membrane was washed with deionized water several times. Drying in a vacuum oven at 60 °C gave QPE-*bl*-5 (or -6) membrane (in chloride form). The QPE-*bl*-5 (or -6) membrane (0.20 g) was dissolved in DMSO (4 mL) and recast onto a flat glass plate. Drying the solution at 60 °C gave a membrane (ca. 50 μm thick). Then, the membrane was treated with 1 M potassium hydroxide aqueous solution at room temperature for 48 h. The membrane was washed and soaked in degassed deionized water for 1 day to obtain a QPE-*bl*-5 (or -6) membrane (in hydroxide form).

Measurements. ^{1}H (500 MHz) and ^{19}F (471 MHz) NMR spectra were obtained on a JEOL JNM-ECA 500 using $CDCl_3$ or DMSO-d_6 as a solvent and TMS as an internal reference. Apparent molecular weights were measured with gel permeation chromatography (GPC) with a Jasco 805 UV detector. DMF containing 0.01 M lithium bromide was used as an eluent. A Shodex K-805L column was used for polymers, and a Shodex SB-803HQ column was used for oligomers, respectively. Molecular weights were calibrated with standard polystyrene samples. For transmission electron microscopic (TEM) observation, the membranes were stained with tetrachloroplatinate ions by ion exchange of the ammonium groups in a 0.5 M potassium tetrachloroplatinate (II) aqueous solution, rinsed with deionized water, and dried in a vacuum oven at 80 °C. The stained membranes were

Scheme 1. Synthesis of QPE-*bl*-5, 6

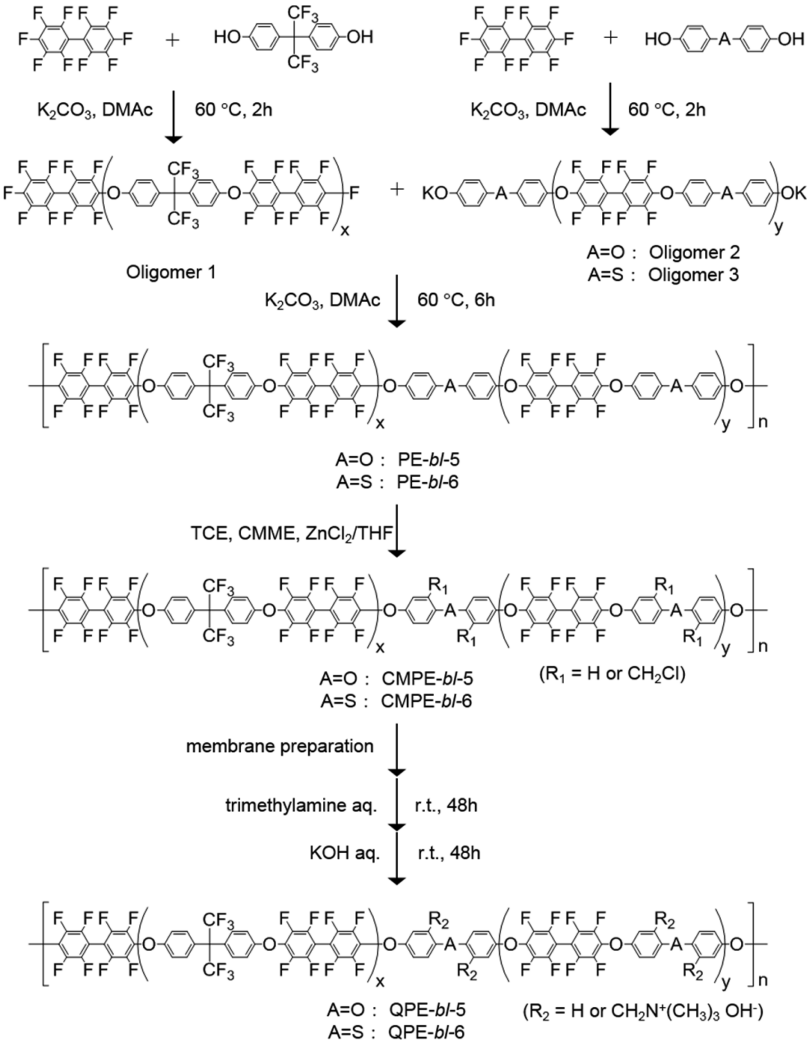

embedded in epoxy resin, sectioned to 50 nm thickness with a Leica microtome Ultracut UCT, and placed on copper grids. Images were taken on a Hitachi H-9500 TEM with an accelerating voltage of 200 kV. Hydroxide ion conductivity of the membranes was measured in a degassed, deionized water (18 MΩ cm) using a four-probe conductivity cell attached with impedance spectroscopy (Solartron 1255B and 1287). Ion conducting resistances (R (Ω)) were determined from the impedance plot obtained in the frequency range from 10 to 10^5 Hz. The hydroxide ion conductivity (σ (S cm^{-1})) was calculated from the equation $\sigma = l/(A \times R)$, where l (cm) and A (cm^2) are the distance between inner two probes and the conducting area, respectively. Water uptake and dimensional change measurements were carried out in deionized water at room temperature for 24 h. Drying the membranes in a vacuum oven at 80 °C provided weight (W_d (g)) and length (D_d (cm)) of dry membranes. Weight and length (D_w (cm)) of wet membranes (W_w (g)) were measured after the surface water was carefully wiped off with tissue paper. The water uptake of the membranes was calculated using the following equation: Water uptake (%) = $(W_w - W_d)/W_d \times 100$. The dimensional change was calculated using the following equation: dimensional change (%) = $(D_w - D_d)/D_d \times 100$. Dynamic mechanical analysis (DMA) was carried out with an ITK DVA-225 dynamic viscoelastic analyzer. Relative humidity (RH) dependence of storage modulus (E' (Pa)), loss modulus (E'' (Pa)), and tan δ at 80 °C was obtained for the membrane (5 mm × 30 mm) at a humidification rate of 1% RH min^{-1}. Hydrogen and oxygen permeability was measured with a GTR Tec GTR-20XFYC gas permeation measurement apparatus equipped with a Yanaco G2700T gas chromatograph (GC) with a thermal conductivity detector. Argon and helium were used as a carrier for the measurement of hydrogen and oxygen, respectively. Membranes were placed in the center of the permeation cell, and the test gas was introduced onto one side of the membrane at a flow rate of 20 mL min^{-1}. Carrier gas was introduced onto the other side of the membrane at the same flow rate and was analyzed by the GC. The same humidity conditions were applied to both test and carrier gases to ensure homogeneous wetting of the membrane samples. Then, 15 mL of flow gas was sampled and subjected to the GC to quantify the test gas permeated through the membrane. The measurement was repeated until stable permeation data were obtained. The gas permeability coefficient of the membranes (Q (cm^3 (STP) cm s^{-1} cm^{-2} cmHg^{-1})) was calculated using the following equation: $Q = 273/T \times 1/A \times B \times 1/t \times d \times 1/(76 - P_{water})$, where T (K) is the absolute temperature, A (cm^2) is the permeation area, B (cm^3) is the volume of the test gas permeated through the membrane, t (s) is the sampling time, d (cm) is the thickness of the membrane, and P_{water} (cmHg) is the water vapor pressure. Hydrazine permeability was determined using an H-type two-compartment cell separated by the membranes. A 10 wt % hydrazine aqueous solution was poured into one compartment, and deionized water was poured into the other compartment on the same level. The solutions were stirred with a magnetic stirring bar to ensure the homogeneity of the solutions. A total of 1 mL of solution was sampled from the deionized water side every hour for 5 h, and 1 mL of fresh deionized water was added each time. The sampled solutions were diluted by 100 times with deionized

water, and the mass of hydrazine in the solutions was quantified with a Metrohm 881 Compact IC ion chromatography. The hydrazine permeability of the membranes (Q' (g mm m^{-2} h^{-1})) was calculated using the following equation: $Q' = m/t \times d \times 1/A$, where m (g) is the mass of hydrazine permeation per hour, t (h) is the sampling time, d (mm) is the thickness of the membrane, and A (m^2) is the permeation area.

Preparation of Catalyst Coated Membrane (CCM) and Fuel Cell Operation. A mixture of NiZn catalysts (0.150 g) and DMF (1.5 mL) was sonicated with a TAITEC VP-50 ultrasonic homogenizer for 10 min. QPE-*bl*-5 (X24Y6, IEC = 0.7 mequiv g^{-1}, 2 wt %) was added to the mixture, which was sonicated for 3 min and stirred with an IKA VIBRAX VXR basic shaker for 15 min. The obtained slurry was sprayed onto one side of a QPE-*bl*-5 membrane (X6Y9, IEC = 1.9 mequiv g^{-1}, 16.0 cm^2) to form the anode catalyst layer. The coated area was 4.41 cm^2. Then, iron phenanthroline (0.050 g) and DMF (2.0 mL) were mixed with an ITOH LA-PO.1 ball mill at 200 rpm for 2 h and sonicated for 60 min. QPE-*bl*-5 (X6Y9, IEC = 1.9 mequiv g^{-1}, 2 wt %) was added to the mixture, which was sonicated for 3 min. A 60 wt % polytetrafluoroethylene dispersion (Daikin, D-210C, 0.0034 g) was added to the mixture and mixed for 15 min. The obtained slurry was sprayed onto the other side of the membrane in a similar way to that described above for the anode catalyst layer. The loaded amounts of the catalysts were 2.6 mg cm^{-2} for NiZn as the anode and 1.0 mg cm^{-2} for iron phenanthroline as the cathode, respectively. The catalyst-coated membrane (CCM) was pressed at 13 MPa at room temperature for 30 s. The CCM was set into a single cell with a gas diffusion layer (anode: cloth, Zoltek and cathode: cloth, Zoltek with microporous layer) and treated with 1.0 M potassium hydroxide aqueous solution overnight for the ion exchange of the membrane and binder to the hydroxide form. A fuel cell was operated at 80 °C, supplying a mixture of 1.0 M potassium hydroxide and 5.0 wt % hydrazine aqueous solution to the anode at a flow rate of 2 mL min^{-1} and humidified air (26%RH) to the cathode at a flow rate of 500 mL min^{-1}. The operating pressure was set at 20 kPa for both electrodes. Serpentine and comb-shaped flow fields were used for the anode and the cathode, respectively.

RESULTS AND DISCUSSION

Synthesis of QPE-*bl*-5, -6. The title quaternized block copolymers, QPE-*bl*-5 and -6, were synthesized as shown in Scheme 1. Hydrophobic oligomers **1** were prepared by nucleophilic substitution polycondensation of DFBP and HFBPA under basic conditions. Slight excess of DFBP was used to obtain fluorine-terminated telechelic oligomers **1** with controlled chain length. The chemical structure of **1** was characterized by ^{1}H and ^{19}F NMR spectra, in which all peaks were well-assigned to the supposed chemical structure (Figure S1a). A detailed discussion on the synthesis and characterization of **1** can be found in our previous report.[15] The numbers of a repeat unit of **1** were estimated from the ^{19}F NMR spectra and GPC analyses (Figure S2, calibrated with polystyrene standards), which were in fair agreement with those expected from the feed comonomer ratios (Table 1).

Table 1. Molecular Weight of Oligomers 1

	x^a	x^b	x^c	$M_n{}^d$/kDa	$M_w{}^d$/kDa	M_w/M_n
oligomer **1**	5	4.4	6.8	4.6	8.4	1.8
	4	5.3	5.4	3.9	6.3	1.6
	8	9.0	10.9	7.2	12.6	1.8
	22	23.9	16.8	10.9	22.3	2.0

[a]Calculated from the feed comonomer ratio. [b]Determined by ^{19}F NMR spectra. [c]Calculated from M_n. [d]Determined by GPC analyses (calibrated with polystyrene standards).

Precursor oligomers **2** and **3** for the hydrophilic blocks were prepared from DFBP and BHPE for **2** or BHPS for **3** under the reaction conditions similar to those for **1**. The chemical structure of **2** and **3** was characterized by ^{1}H and ^{19}F NMR spectra (Figure S1b). In the ^{1}H NMR spectra of oligomers **2** and **3**, the small peaks at 6.7−7.3 ppm were assignable to the terminal bisphenol groups. The ^{19}F NMR spectra of oligomers **2** and **3** showed two large peaks at −137.9 and −153.0 ppm, suggesting that the reaction of DFBP occurred preferentially at its 4,4′-positions to give the linear oligomers **2** and **3**. In the ^{19}F NMR spectra of oligomers **2** and **3**, no peaks derived from DFBP-terminal were confirmed, indicating complete end-capping with hydroxyl-containing monomers (BHPE or BHPS). The numbers of repeat units of **2** and **3** were estimated from the ^{1}H NMR spectra and GPC analyses (Figure S2), which were somewhat greater than those expected from the feed comonomer ratios (Table 2), probably due to slightly lower reactivity of BHPE and BHPS compared to HFBPA.

Table 2. Molecular Weight of Oligomers 2 and 3

	y^a	y^b	y^c	$M_n{}^d$/kDa	$M_w{}^d$/kDa	M_w/M_n
oligomer **2**	4	6.4	9.2	4.8	8.4	1.7
	4	7.0	8.1	4.4	7.4	1.7
	8	7.9	13.6	7.0	15.5	2.2
	8	11.3	10.7	6.7	24.5	3.7
oligomer **3**	4	6.8	10.6	5.7	10.4	1.8
	4	8.0	7.0	3.8	5.9	1.6

[a]Calculated from the feed comonomer ratio. [b]Determined by ^{1}H NMR spectra. [c]Calculated from M_n. [d]Determined by GPC analyses (calibrated with polystyrene standards).

PE-*bl*-5 and -6 were synthesized via block copolymerization of the oligomers **1** and **2** or **3** under conditions similar to those for the above-mentioned oligomers. The molecular weight calculated from the NMR spectra was used for calculation of the feed oligomer ratio. Block copolymerization reactions were carried out at low temperature (60 °C) and short time (8 h) to avoid unfavorable side reactions such as cross-linking or branching. The obtained PE-*bl*-5 and -6 were soluble in organic solvents such as chloroform, TCE, DMSO, DMAc, and DMF. PE-*bl*-5 and -6 were characterized by ^{1}H and ^{19}F NMR spectra, which suggested the equimolar components of the starting oligomers (Figure 1a and Figure S3a). There was no detectable evidence of the terminal groups and unfavorable side reactions. The molecular weights of PE-*bl*-5 and -6 were M_n = 18−70 kDa and M_w = 61−263 kDa, respectively (Table 3), which were several times greater than those of the starting oligomers to support the formation of the multiblock copolymers. It should be noted that the apparent molecular weights obtained by GPC analyses with polystyrene standards could be overestimated since PEs as typical aromatic polymers would not form a typical random coil configuration in the GPC eluents (DMF containing 0.01 M LiBr, Figure S4).

A Friedel−Crafts chloromethylation reaction of the PE-*bl*-5 and -6 with CMME was carried out using zinc chloride as a Lewis acid catalyst in TCE solution. CMPE-*bl*-5 and -6 showed slightly better solubility than the parent PE-*bl*-5 and -6 and were soluble in chloroform, TCE, DMAc, DMF, and DMSO. In the ^{1}H NMR spectra of CMPE-*bl*-5 and -6, a new peak (peak 8) appeared at 4.7 ppm assignable to the chloromethyl groups. The peaks 3 and 4 were smaller than those of the precursor PE-*bl*-5 and -6 (Figure 1b and Figure S3b). The results indicate

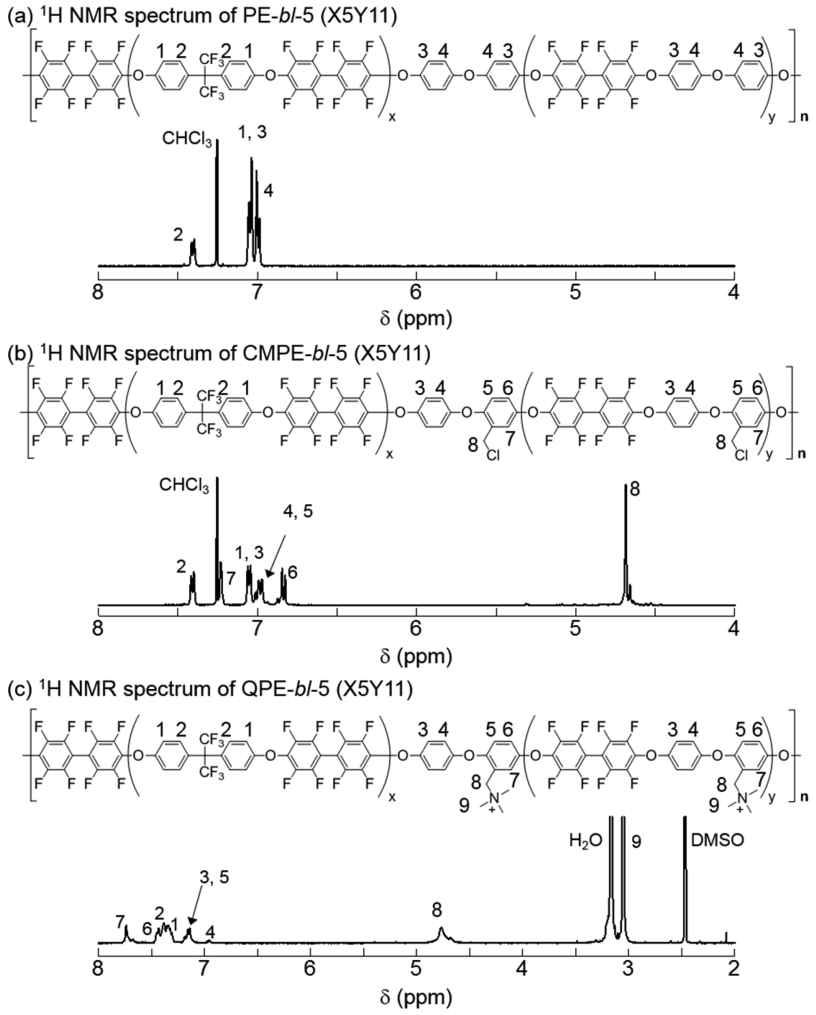

Figure 1. ^{1}H NMR spectra of (a) PE-*bl*-5 (X5Y11) in $CDCl_3$, (b) CMPE-*bl*-5 (X5Y11) in $CDCl_3$, and (c) QPE-*bl*-5 (X5Y11) in DMSO-d_6 at room temperature.

Table 3. Properties of PE-*bl*, CMPE-*bl*, and QPE-*bl*-5 and -6

	molecular weight			
	M_n[a]/kDa	M_w[a]/kDa	DC[b]	IEC[c]/meq g^{-1}
QPE-*bl*-5 (X5Y11)	29	127	2.1	2.1
QPE-*bl*-5 (X9Y8)	64	277	2.1	1.5
QPE-*bl*-5 (X4Y7)	18	61	1.9	1.3
QPE-*bl*-5 (X4Y7)	18	61	1.4	1.0
QPE-*bl*-5 (X24Y6)	70	232	2.1	0.7
QPE-*bl*-6 (X4Y8)	21	97	1.8	1.3
QPE-*bl*-6 (X4Y8)	21	97	1.2	1.0
QPE-*bl*-6 (X24Y7)	59	263	1.9	0.7

[a]Determined by GPC analyses (calibrated with polystyrene standards). [b]Degree of chloromethylation = (amount of chloromethyl group/repeat unit), calculated from ^{1}H NMR spectra. [c]Expected IECs calculated from ^{1}H NMR spectra.

that the chloromethyl groups were substituted onto the main-chain phenylene rings at both positions ortho and meta to the ether groups, probably due to their similar electron densities and steric situations.[16] The degree of chloromethylation in CMPE-*bl*-5 was higher than that of CMPE-*bl*-6 under the same reaction conditions. In our previous polymers containing fluorenylidene biphenyl groups, the chloromethyl groups could not be substituted at the main-chain phenylene rings but only on the fluorenyl groups.[15] In the present polymers, the main chain phenylene groups were chloromethylated because of the strong electron-donating chalcogen (ether and sulfide) groups. In the ^{19}F NMR spectra of CMPE-*bl*-5 and -6, the peak at −64.0 ppm assignable to trifluoromethyl groups appeared at the same chemical shift to those of the precursor PE-*bl*-5 and -6. The result is indicative that no chloromethylation occurred at the phenylene rings bonded with electron-withdrawing trifluoromethyl groups in the hydrophobic blocks. The degree of chloromethylation was estimated from the integral ratios of the peaks of chloromethyl groups (peak 8) to the peaks of phenylene protons ortho to the hexafluoropropyl groups (peak 2) in the ^{1}H NMR spectra. As summarized in Table 4, the degree of chloromethylation increased with the reaction time and temperature and the amount of CMME. A nearly quantitative chloromethylation reaction (each phenylene ring in diphenyl ether and diphenyl sulfide groups was chloromethylated) was achieved. GPC profiles (Figure S4) were unimodal and shifted to lower retention time (higher molecular weight) compared to those of the starting PE-*bl*-5 and -6. The ^{1}H and ^{19}F NMR spectra and GPC profiles of the CMPE-*bl*-5 and -6 suggested no detectable evidence of degradation and cross-linking during the chloromethylation reaction.

Casting from the TCE solution of CMPE-*bl*-5 and -6 provided colorless, transparent, and bendable membranes. The

Table 4. Degree of Chloromethylation in PE-*bl*-5 and -6

	temperature/°C	CMME[a]	reaction time/h	DC[b]
PE-*bl*-5 (X4Y7)	50	80	48	0.8
	50	80	120	1.0
	50	160	48	1.3
	80	80	48	1.3
	80	80	120	1.4
	80	160	120	1.9
PE-*bl*-6 (X4Y8)	50	80	48	0.3
	50	80	120	0.6
	50	160	48	0.6
	80	80	48	0.7
	80	80	120	0.8
	80	160	120	1.8

[a]Equivalent vs repeat unit. [b]Degree of chloromethylation = (amount of chloromethyl group/repeat unit), calculated from ^{1}H NMR spectra.

membranes were quaternized by treating with trimethylamine aqueous solution. A series of QPE membranes with ion exchange capacity (IEC) values ranging from 0.7 to 2.1 mequiv g^{-1} were obtained. The as-prepared QPE-*bl*-5 and -6 membranes were light brown and less flexible compared with the parent CMPE membranes. Unlike our previous QPEs with quaternized fluorenyl groups,[7,14,15] the obtained QPE-*bl*-5 and -6 were soluble in polar organic solvents such as DMSO and DMF, which enabled recasting the membranes. The flexibility (bendability) of the membranes was recovered by recasting from DMSO solutions. In the ^{1}H NMR spectra of QPE-*bl*-5 and -6, new peaks (peak 9) appeared at 4.8 ppm assignable to the methyl groups on quaternary ammonium groups (Figure 1c and Figure S3c). The peaks 8 shifted to a higher magnetic field compared to those of CMPE-*bl*-5 and -6, indicating complete quaternization of the chloromethyl groups in CMPE-*bl*-5 and -6. GPC analyses were unavailable because of the possible interactions of the quaternized polymers with our GPC columns. The difference in the hydrophilic block (diphenyl sulfide and diphenyl ether) had a minor effect on the syntheses.

Morphology and Properties of QPE-*bl*-5 and -6 Membranes. Figure 2 shows cross-sectional TEM images of QPE-*bl*-5 and -6 (in tetrachloroplatinate form), in which the dark areas represent ionic clusters composed of ammonium tetrachloroplatinate groups and the bright areas represent hydrophobic moieties composed of polymer main chains. QPE-*bl*-5 and QPE-*bl*-6 membranes displayed distinct phase-separated morphology similar to those of our partially fluorinated QPE membranes with comparable IEC.[15] The hydrophilic domains were ca. 5 nm wide and interconnected throughout the field of view. The two membranes with the same IEC values (Figure 2a and c) showed similar morphology, indicating that the chalcogen bonds in the hydrophilic blocks did not impact the phase-separated morphology. The QPE-*bl*-5 membrane with higher IEC (Figure 2b) did not provide more developed phase separation, indicating that IEC showed a minor effect. The phase-separated morphology was not as distinct as those of our previous quaternized multiblock poly(arylene ether)s containing fluorenyl groups in the hydrophilic block, while the latter was quaternized after the casting. It is considered that bulky fluorenyl groups could contribute to development of the phase-separated morphology. Similar results were obtained in our proton conducting membranes.[17,18]

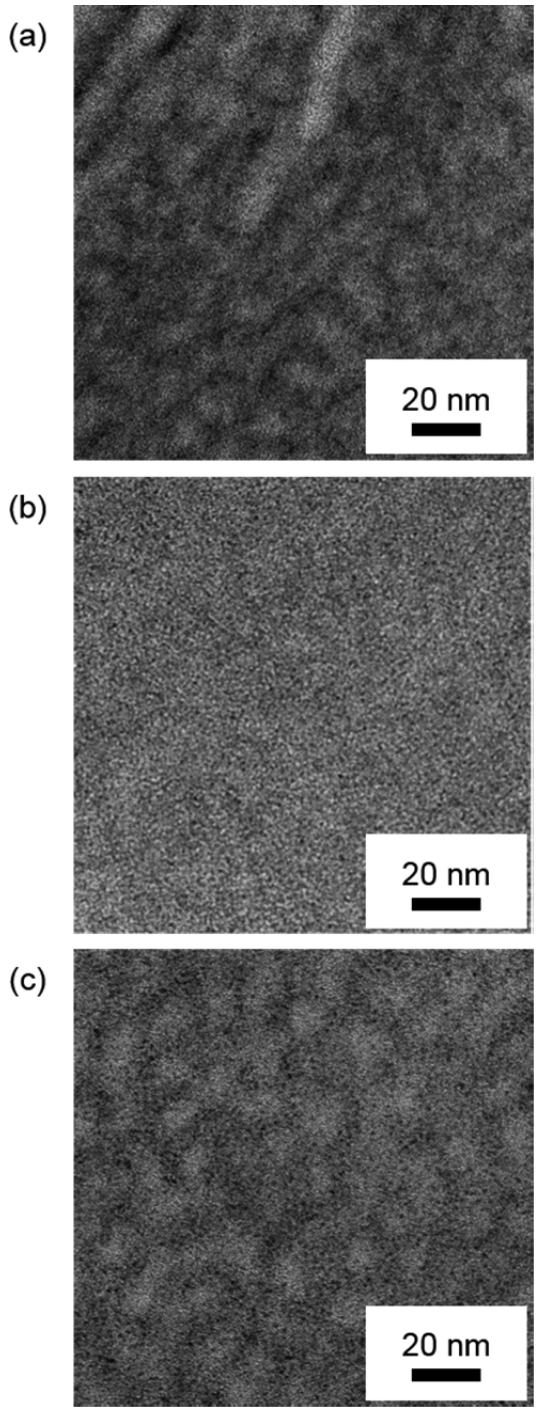

Figure 2. TEM images of (a) QPE-*bl*-5 (X4Y7, IEC = 1.3 mequiv g^{-1}), (b) QPE-*bl*-5 (X5Y11, IEC = 2.1 mequiv g^{-1}), and (c) QPE-*bl*-6 (X4Y8, IEC = 1.3 mequiv g^{-1}) membranes stained with tetrachloroplatinate ions.

Water uptake at room temperature and hydroxide ion conductivity at 60 °C of QPE-*bl*-5 and -6 membranes were measured and are plotted as a function of the IEC in Figure 3. Water uptake of QPE-*bl*-5 and -6 membranes increased with increasing IEC values as expected. The number of absorbed water molecules per ammonium group (λ) followed the same tendency and was in approximate linear relationship with the IEC value (Figure S5). The connecting chalcogen groups, ether or sulfide, did not affect the water absorbing properties of the

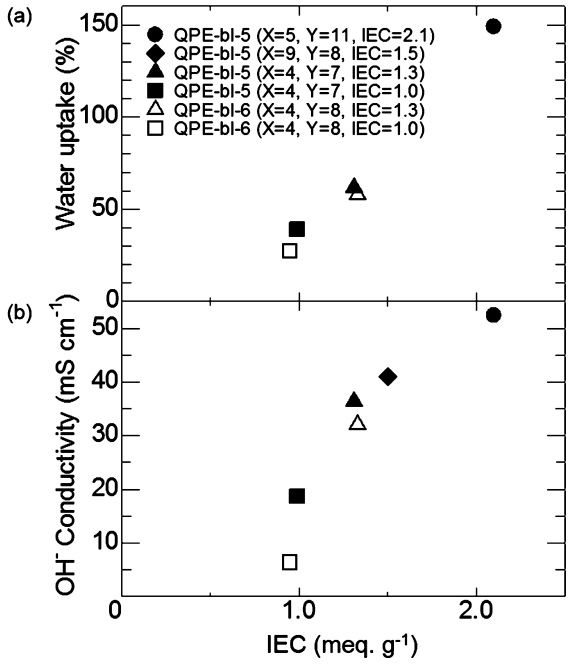

Figure 3. (a) Water uptake at room temperature and (b) hydroxide ion conductivity at 60 °C of QPE-*bl*-5 and -6 membranes as a function of IEC.

QPE membranes. In the QPE-*bl*-5 membrane (2.1 mequiv g^{-1}), in-plane and through-plane dimensional changes were 27% and 12%, respectively. QPE-*bl*-5 membranes showed slightly higher hydroxide ion conductivity than that of QPE-*bl*-6 membranes with comparable IEC. The local IEC value in the hydrophilic block was higher for QPE-*bl*-5 (2.9 mequiv g^{-1}) than for QPE-*bl*-6 (2.7 mequiv g^{-1}), which could account for the higher ion conductivity of QPE-*bl*-5 membranes. Temperature dependence of hydroxide ion conductivity of QPE-*bl*-5 and -6 membranes is shown in Figure 4. The hydroxide ion

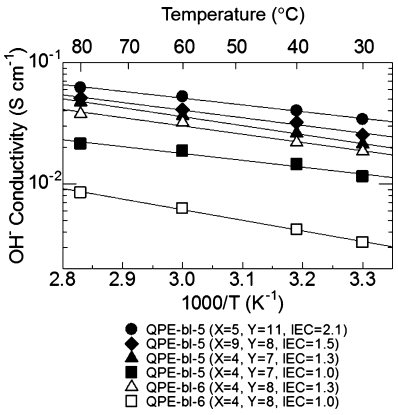

Figure 4. Temperature dependence of hydroxide ion conductivities of QPE-*bl*-5 and -6 membranes.

conductivity of QPE-*bl*-5 and -6 membranes increased with increasing temperature, and QPE-*bl*-5 with the highest IEC (2.1 mequiv g^{-1}) achieved 62 mS cm^{-1} at 80 °C. While this conductivity was very high, QPE-*bl*-5 and -6 membranes exhibited relatively low hydroxide ion conductivity compared to those of our poly(arylene ether) block copolymer membranes containing ammonium-substituted fluorenyl groups (45 mS cm^{-1} for QPE-*bl*-4, IEC = 1.3 mequiv g^{-1} at 80 °C) taking the IEC values into account.[15] The results may imply that bulky fluorenyl groups serve better as a scaffold for ionic groups than the slightly bent diphenyl ether and sulfide groups. The hydroxide ion conductivity of the QPE-*bl*-5 and -6 membranes showed approximate Arrhenius-type temperature dependence. The apparent activation energies were estimated from the slopes to be 11−17 kJ mol^{-1}, which were similar to those of our previous QPEs,[15] indicating that they share similar ion-conducting mechanism involving hydrated hydroxide ions. Since QPE-*bl*-5 exhibited higher hydroxide ion conductivity than that of QPE-*bl*-6, we focused on the QPE-*bl*-5 membrane for further investigation below.

An alkaline stability test of the QPE-*bl*-5 membrane (IEC = 1.0 mequiv g^{-1}, in chloride form) was carried out in 1 M KOH aqueous solution at 40 °C (Figure 5). The QPE-*bl*-5 membrane

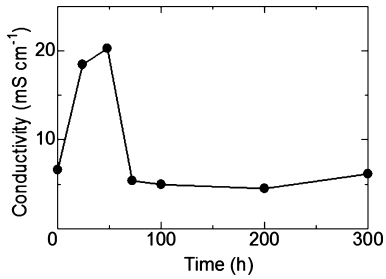

Figure 5. Time course of ion conductivity of QPE-*bl*-5 membrane (IEC = 1.0 mequiv g^{-1}) in 1 M KOH aqueous solution at 40 °C.

exhibited an initial conductivity of 6.6 mS cm^{-1}. The conductivity increased to 20.1 mS cm^{-1} within 48 h since the anions were exchanged from chlorides to more conductive hydroxides. Then, the conductivity dropped to ca. 5.4 mS cm^{-1} after 72 h and maintained a nearly constant value up to 300 h. The post-test analysis was conducted with a ^{1}H NMR spectrum (Figure S6). While the integral ratios of the peaks of all aromatic protons (both hydrophilic and hydrophobic segments) to methylene groups (peak 8) or methyl groups (peak 9) did not change after a 300 h stability test, there were small changes in the aromatic protons associated with benzylammonium groups. In the ^{19}F NMR spectrum of the post-test sample, the peaks assignable to octafluorobiphenylene groups became smaller and new peaks appeared nearby. The results indicate that QPE-*bl*-5 degraded to a small extent during the stability test most probably in the hydrophilic blocks, which was accountable for the decrease in the hydroxide ion conductivity. The degradation after 300 h was not significant as confirmed by high conductivity (ca. 6 mS cm^{-1}) and bendability of the post-test membrane.

Hydrogen and oxygen permeability of QPE-*bl*-5 membrane (X9Y8, IEC = 1.5 mequiv g^{-1} (in chloride form)) was measured at 80 °C and plotted as a function of RH in Figure 6. The hydrogen and oxygen permeability coefficients of the QPE-*bl*-5 membrane were 3.3 × 10^{-9} cm^3 (STP) cm s^{-1} cm^{-2} $cmHg^{-1}$ and 4.9 × 10^{-10} cm^3 (STP) cm s^{-1} cm^{-2} $cmHg^{-1}$, respectively, at 30% RH. The hydrogen permeability coefficient was nearly constant at any humidity examined, while the oxygen permeability coefficient increased slightly with RH. Such differences between hydrogen and oxygen may arise from the affinity of oxygen to the fluorinated polymer main chains. The gas (especially, oxygen) permeability coefficients of the QPE-*bl*-5 membrane were slightly higher than those of our

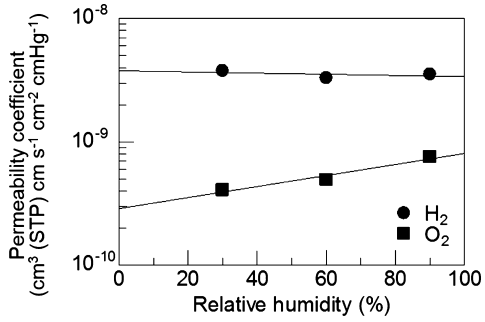

Figure 6. Hydrogen and oxygen permeability of the QPE-*bl*-5 membrane (IEC = 1.5 mequiv g^{-1}) at 80 °C as a function of RH.

aromatic PEMs.[19] Fluorinated main chains in QPE-*bl*-5 may be responsible for higher gas permeability. Compared with the large water uptake values (Figure 3), the humidity dependence of the gas permeabilities of the membrane was much less significant, indicating that the gases permeate mainly through the hydrophobic domains of the QPE-*bl*-5 membrane.

Taking into account the direct hydrazine fuel cell applications, hydrazine permeabilities of QPE-*bl*-5 and -6 membranes were measured and plotted as a function of IEC in Figure 7. The hydrazine permeability coefficient was negligibly

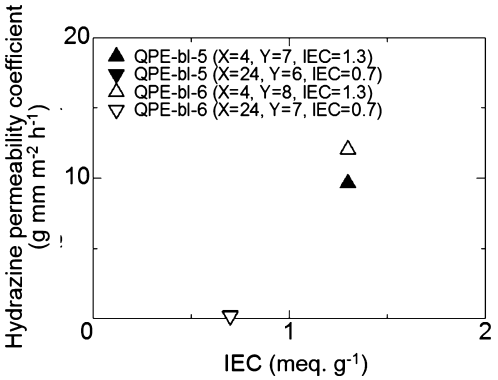

Figure 7. Hydrazine permeability of QPE-*bl*-5, -6 membranes as a function of IEC.

small (<0.24 g mm m^{-2} h^{-1}) for the low IEC (0.7 mequiv g^{-1}) membranes. High IEC (1.3 mequiv g^{-1}) membranes were more hydrazine permeable with the coefficients of ca. 10 g mm m^{-2} h^{-1}. The results are reasonable taking the hydrophilic nature of hydrazine into account.

As a mechanical stability test, humidity dependence of the storage modulus (E'), loss modulus (E''), and tan δ (E''/E') of the QPE-*bl*-5 membrane (X9Y8, IEC = 1.5 mequiv g^{-1} (in chloride form)) was measured at 80 °C as shown in Figure 8. The E' value gradually decreased with increasing the humidity, suggesting that the absorbed water in the membrane acted as a plasticizer. The QPE-*bl*-5 membrane showed a greater E' value than 1.3×10^8 Pa under a wide range of humidity (ca. 0–90% RH), which was comparable to that of our poly(arylene ehter)-based PEMs.[17,19] The results indicate that not the ionic (sulfonic acid or ammonium) groups but the main chain structure is a more decisive factor in dynamic mechanical properties of the aromatic ionomer membranes. E', E'', and tan δ curves exhibited no distinct transitions, suggesting that the QPE-*bl*-5 membrane was mechanically stable under fuel cell operating conditions associated with humidity changes.

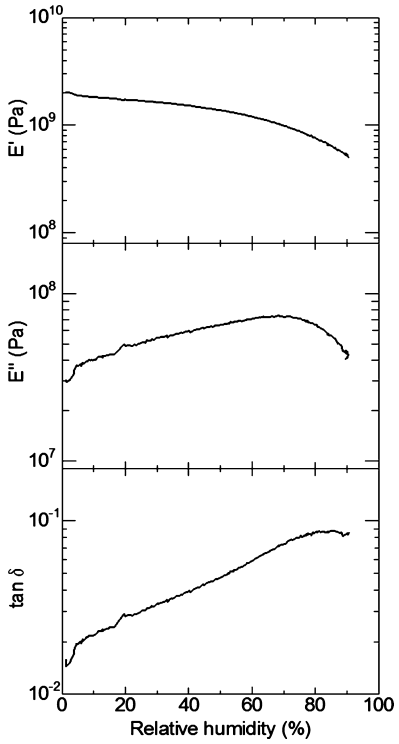

Figure 8. DMA analysis of the QPE-*bl*-5 (IEC = 1.5 mequiv g^{-1}) membrane at 80 °C as a function of RH.

Since QPE-*bl*-5 and -6 showed reasonable solubility in polar organic solvents, they could be utilized as electrode binders and the membranes for a platinum-free fuel cell. QPE-*bl*-5 (X6Y9, IEC = 1.9 mequiv g^{-1}) was used as the membrane and the cathode binder, while QPE-*bl*-5 (X24Y6, IEC = 0.7 mequiv g^{-1}) with a lower IEC was used as the anode binder. Since hydrazine aqueous solution was supplied to the anode, a low IEC ionomer was used for the anode binder to prevent excessive swelling and hydrazine permeation. A direct hydrazine fuel cell was operated with an MEA using QPE-*bl*-5 as the membrane and the electrode binder at 80 °C (Figure 9). The

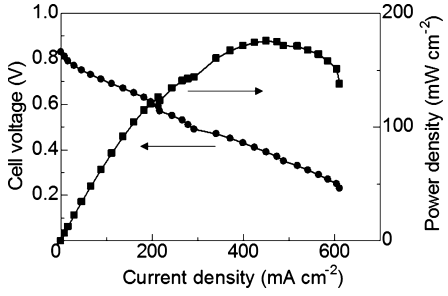

Figure 9. Direct hydrazine fuel cell performance of an MEA with QPE-*bl*-5 membrane and electrode binder at 80 °C.

open circuit voltage (OCV) was 0.83 V, which was higher than that of our previous AEM (0.71 V), indicative of lower hydrazine permeability of the QPE-*bl*-5 membrane. The maximum power density of 176 mW cm^{-2} was achieved at a current density of 451 mA cm^{-2} with air. This value was also slightly superior to those of our previous AEM (maximum power density was 161 mW cm^{-2} at 446 mA cm^{-2}).[7]

dx.doi.org/10.1021/am5046586 | ACS Appl. Mater. Interfaces 2014, 6, 17044–17052

CONCLUSION

We have designed and synthesized a novel series of quaternized poly(arylene ether) polymers for AEMFCs. The polymers consist of chemically stable fluorinated poly(arylene ether)s and diphenyl ether (QPE-*bl*-5) or diphenyl sulfide (QPE-*bl*-6) groups as a scaffold for quaternized ammonium groups. The QPE membranes showed phase-separated morphology somewhat less developed compared with our previous AEMs containing fluorene groups, indicating bulky cardo groups were effective in developing phase-separated morphology. The chalgcogen bonds, ether or sulfide, did not provide significant differences in the quaternized block copolymer membranes while ether containing QPE-*bl*-5 was somewhat more hydroxide ion conductive than sulfide-containing QPE-*bl*-6. Reasonable alkaline stability of the QPE-*bl*-5 membrane was confirmed in KOH aqueous solution up to 300 h. The QPE-*bl*-5 membrane exhibited high mechanical strength and its low humidity dependence, and low gas and hydrazine permeability. A noble metal-free direct hydrazine fuel cell with QPE-*bl*-5 as the electrode binder and membrane was successfully operated to achieve high maximum power density (176 mW cm^{-2}) at a current density of 451 mA cm^{-2}. The high OCV value confirmed its low hydrazine permeability.

ASSOCIATED CONTENT

Supporting Information

Detailed characterization of oligomers **1**, **2** and PE-*bl*-5, PE-*bl*-6, CMPE-*bl*-6, and QPE-*bl*-6. λ of QPE-*bl*-5 and -6 membranes. This material is available free of charge via the Internet at http://pubs.acs.org/.

AUTHOR INFORMATION

Corresponding Author

*Tel.: +81 552208707. Fax: +81 552208707. E-mail: miyatake@yamanashi.ac.jp.

Notes

The authors declare no competing financial interest.

REFERENCES

(1) Hickner, M.; Herring, A.; Coughlin, B. Anion Exchange Membranes: Current Status and Moving Forward. *J. Polym. Sci., Part B: Polym. Phys.* **2013**, *51*, 1727−1735.
(2) Merle, G.; Wessling, M.; Nijmeijer, K. Anion Exchange Membranes for Alkaline Fuel Cells: A Review. *J. Membr. Sci.* **2011**, *377*, 1−35.
(3) Couture, G.; Alaaeddine, A.; Boschet, F.; Ameduri, B. Polymeric Materials as Anion-Exchange Membranes for Alkaline Fuel Cells. *Prog. Polym. Sci.* **2011**, *36*, 1521−1557.
(4) Park, A. M.; Turley, F. E.; Wycisk, R. J.; Pintauro, P. N. Electrospun and Cross-Linked Nanofiber Composite Anion Exchange Membranes. *Macromolecules* **2014**, *47*, 227−235.
(5) Si, Z.; Qiu, L.; Dong, H.; Gu, F.; Li, Y.; Yan, F. Effects of Substituents and Substitution Positions on Alkaline Stability of Imidazolium Cations and Their Corresponding Anion-Exchange Membranes. *ACS Appl. Mater. Interfaces* **2014**, *6*, 4346−4355.
(6) Noonan, K. J. T.; Hugar, K. M.; Kostalik, H. A.; Lobkovsky, E. B.; Abruña, H. D.; Coates, G. W. Phosphonium-Functionalized Polyethylene: A New Class of Base-Stable Alkaline Anion Exchange Membranes. *J. Am. Chem. Soc.* **2012**, *134*, 18161−18164.
(7) Tanaka, M.; Fukasawa, K.; Nishino, E.; Yamaguchi, S.; Yamada, K.; Tanaka, H.; Bae, B.; Miyatake, K.; Watanabe, M. Anion Conductive Block Poly(arylene ether)s: Synthesis, Properties, and Application in Alkaline Fuel Cells. *J. Am. Chem. Soc.* **2011**, *133*, 10646−10654.
(8) Hwang, G.-J.; Ohya, H. Preparation of Anion-Exchange Membrane Based on Block Copolymers Part 1. Amination of the Chloromethylated Copolymers. *J. Membr. Sci.* **1998**, *140*, 195−203.
(9) Wang, G.; Weng, Y.; Chu, D.; Chen, R.; Xie, D. Developing a Polysulfone-Based Alkaline Anion Exchange Membrane for Improved Ionic Conductivity. *J. Membr. Sci.* **2009**, *332*, 63−68.
(10) Li, X.; Yu, Y.; Liu, Q.; Meng, Y. Synthesis and Properties of Anion Conductive Ionomers Containing Tetraphenyl Methane Moieties. *ACS Appl. Mater. Interfaces* **2012**, *4*, 3627−3635.
(11) Li, X.; Yu, Y.; Meng, Y. Novel Quaternized Poly(arylene ether sulfone)/Nano-ZrO2 Composite Anion Exchange Membranes for Alkaline Fuel Cells. *ACS Appl. Mater. Interfaces* **2013**, *5*, 1414−1422.
(12) Thomas, O.; Soo, K.; Peckham, T.; Kulkarni, M.; Holdcroft, S. A Stable Hydroxide-Conducting Polymer. *J. Am. Chem. Soc.* **2012**, *134*, 10753−10756.
(13) Wright, A.; Holdcroft, S. Hydroxide-Stable Ionenes. *ACS Macro Lett.* **2014**, *3*, 444−447.
(14) Li, N.; Yongjun Leng, Y.; Hickner, M.; Wang, C.-Y. Highly Stable, Anion Conductive, Comb-Shaped Copolymers for Alkaline Fuel Cells. *J. Am. Chem. Soc.* **2013**, *135*, 10124−10133.
(15) Ono, H.; Miyake, J.; Bae, B.; Watanabe, M.; Miyatake, K. Synthesis and Properties of Partially Fluorinated Poly(arylene ether) Block Copolymers Containing Ammonium Groups as Anion Conductive Membranes. *Bull. Chem. Soc. Jpn.* **2013**, *86*, 663−670.
(16) Miyake, J.; Fukasawa, K.; Watanabe, M.; Miyatake, K. Effect of Ammonium Groups on the Properties and Alkaline Stability of Poly(arylene ether)-Based Anion Exchange Membranes. *J. Polym. Sci., Part A: Polym. Chem.* **2014**, *52*, 383−389.
(17) Miyatake, K.; Hirayama, D.; Bae, B.; Watanabe, M. Block Poly(arylene ether sulfone ketone)s Containing Densely Sulfonated Linear Hydrophilic Segments as Proton Conductive Membranes. *Polym. Chem.* **2012**, *3*, 2517−2522.
(18) Bae, B.; Miyatake, K.; Watanabe, M. Sulfonated Poly(arylene ether sulfone ketone) Multiblock Copolymers with Highly Sulfonated Block. Synthesis and Properties. *Macromolecules* **2010**, *43*, 2684−2691.
(19) Hoshi, T.; Bae, B.; Watanabe, M.; Miyatake, K. Synthesis and Properties of Sulfonated Poly(arylene ether) Block Copolymers as Proton Conductive Membranes. *Bull. Chem. Soc. Jpn.* **2012**, *85*, 389−396.